applied sciences

MDPI

Article

Electronic, Optical and Thermoelectric Properties of Two-Dimensional Molybdenum Carbon Mo_2C-MXenes

Doan Thi Kieu Anh [1,2], Pham Hong Minh [1,*], Kohei Yamanoi [3], Marilou Cadatal-Raduban [3,4,*], Luong Viet Mui [5], Do Minh Hieu [1] and Nguyen Dai Hung [1]

[1] Institute of Physics, Vietnam Academy of Science and Technology, 10 Dao Tan, Ba Dinh, Hanoi 100000, Vietnam; kieuanh@iop.vast.vn (D.T.K.A.); minhhieu@iop.vast.vn (D.M.H.); daihung@iop.vast.vn (N.D.H.)
[2] Faculty of Physics, Graduate University of Science and Technology, Vietnam Academy of Science and Technology, 18 Hoang Quoc Viet, Cau Giay, Hanoi 100000, Vietnam
[3] Institute of Laser Engineering, Osaka University, 2-6 Yamadaoka, Suita 565-0871, Osaka, Japan; yamanoi.kohei.ile@osaka-u.ac.jp
[4] Unitec Institute of Technology, 139 Carrington Road, Mount Albert, Auckland 1025, New Zealand
[5] Graduate School of Engineering, Osaka University, 2-1 Yamadaoka, Suita 565-0871, Osaka, Japan; vietmuiluong@gmail.com
* Correspondence: phminh@iop.vast.vn (P.H.M.); mraduban@gmail.com (M.C.-R.)

Abstract: We investigate the structural, electronic, optical, and thermoelectric properties of three compositions of Mo_2C-MXenes (Mo_2CF_2, $Mo_2C(OH)_2$, and Mo_2CO_2) from monolayer to multilayer by first principles calculation within Density Functional Theory (DFT) and Boltzmann transport theory. Firstly, the atomic structures of Mo_2C-MXenes are optimized, and their respective structures are created with comparative research. Secondly, their electronic band structures and optical properties are studied in detail. The estimation of the bandgap energy of Mo_2C-MXenes with its functionalization reveal that most Mo_2CF_2 and $Mo_2C(OH)_2$ layers are semiconductors, while Mo_2CO_2 behaves as a metal. The electrical and optical properties can be altered by controlling the on-surface functional groups and the number of layers. Computation of the thermoelectric (TE) properties of Mo_2C-MXenes reveals that, upon heating to 600 K, Mo_2CF_2 and $Mo_2C(OH)_2$ exhibit a high Seebeck coefficient and a relatively high electrical conductivity. The Seebeck coefficient reaches ~400 μV K^{-1} at room temperature for all layers of Mo_2CF_2 MXenes. Our results prove that Mo_2CF_2 is considered a promising material for thermoelectric devices, while Mo_2CO_2 does not possess better thermoelectric performance. Mo_2C-MXenes from monolayer to multilayer have outstanding properties, such as flexible bandgap energy and high thermal stability, making them promising candidates for many applications, including energy storage and electrode applications.

Keywords: 2D materials; Mo_2C-MXenes; electronic band structure; optical properties; thermoelectric properties

Citation: Anh, D.T.K.; Minh, P.H.; Yamanoi, K.; Cadatal-Raduban, M.; Mui, L.V.; Hieu, D.M.; Hung, N.D. Electronic, Optical and Thermoelectric Properties of Two-Dimensional Molybdenum Carbon Mo_2C-MXenes. *Appl. Sci.* **2024**, *14*, 9257. https://doi.org/10.3390/app14209257

Academic Editor: Roberto Bergamaschini

Received: 11 September 2024
Revised: 7 October 2024
Accepted: 9 October 2024
Published: 11 October 2024

1. Introduction

Since the first successful preparation of graphene in 2004 [1], two-dimensional (2D) materials have attracted great attention owing to their unique properties and potential applications in areas such as energy storage, catalysis, and electronics [2–4]. In 2011, Gogotsi, Barsoum and other researchers [5] introduced a novel group of 2D transition metal carbides, nitrides, and carbon nitrides known as MXenes, which has rapidly spurred the exploration of new 2D materials in the field of materials science. In general, MXenes have been synthesized by using strong acid or alkali solutions [6] and exfoliating their A-layers in the MAX phases [7,8], where M is an early transition metal (M: Mo, Ti, Zr, Cr, W, ...), A is a group element (A: Si, Ga, Al, ...), and X is a carbon and/or nitrogen atom (X: C, N). This formed transition metal carbides and nitrides with the $M_{n+1}X_nT_x$ formula, where T

represents functional groups such as F, H, O, or OH and n = 1, 2, 3, or 4 [9,10]. To date, over 70 different synthesized MAX phases have been reported [11]. Thus far, the addition of termination groups (T) on the MXene surface has resulted in more than 30 distinct MXenes structures being experimentally obtained and theoretically predicted [12,13].

In recent years, 2D MXenes, including $Ti_3C_2T_x$, Nb_2CT_x, Mo_2CT_x [14–16], etc., have been explored in every possible field, with particular attention paid to energy storage applications, mainly due to their good electrical conductivity and ability to host of cations (e.g., Li^+ and Na^+). Compared with the common MXenes, Mo_2C-MXenes are new and stand out from various MXenes. They were successfully obtained by the selective etching of Ga layers from Mo_2Ga_2C MAX phases using hydrofluoric acid [16–18]. The current studies show that Mo_2C-structures have high storage capacity, excellent electrical conductivity, chemical stability, and other properties, making them potential electrocatalysts [19], photocatalysts for photocatalytic H_2 production [20,21], anode materials in batteries [9], and materials for electromagnetic interference shielding [22]. Interestingly, among 35 different functionalized MXenes, Mo_2CT_x functionalized with fluoride (F) has been reported to have an excellent thermoelectric power factor [23]. Generally, the etching solution used in the synthesis process is directly related to the type of surface termination. Therefore, the electronic and optical properties of MXenes are strongly dependent on the interaction between the outer metal layer and the surface functional groups (F, OH, O, Cl, etc.). However, there is a lack of information about the dependence of the electronic, optical, and thermoelectric properties of Mo_2C-based MXenes materials on the surface termination groups and the number of layers. As a material with a small bandgap, knowing how the number of layers affects the electronic, optical, and thermoelectric properties will greatly enhance its potential. Therefore, we investigated these properties for three kinds of Mo-based MXenes, namely, Mo_2CF_2, $Mo_2C(OH)_2$, and Mo_2CO_2, with different structures, from monolayer to multilayer. Knowledge of the properties of Mo_2C-MXenes resulting from this work will guide experiments and the development of new applications using Mo_2C-MXenes.

2. Computational Methods

All calculations were performed within the framework of density functional theory, as implemented in the VASP code [24]. The generalized gradient approximation (GGA) of Perdew–Burke–Ernzerhof (PBE) was used as the exchange correlation functional. The plane wave cut-off energy was set to 520 eV. The electronic structures were calculated using 41 × 41 × 1 Monkhorst-Pack *k*-point sampling for Mo_2CT_2, where T represents surface functional groups (O, OH, and F). The 1 × 1 × 1 unit cell of a bulk crystal was selected on the basis of previous calculations [23]. The monolayers and multilayers were constructed by adding a layer into the 1 × 1 × 5 supercell in VESTA and were optimized when a layer was added. The optimized lattice constants and bond lengths are shown in Table 1. The electronic structures were calculated along the highly symmetric k-points line *G–A–H–K–G–M–L–H* in the first Brillouin zone.

The optical properties of MXenes have a high dependence on the energy structure, specifically on the bandgap energy and the type of bandgap (direct or indirect). In addition, the optical properties are related to the dielectric function, which is described by the optical frequency (ω), and the real and imaginary part as follows:

$$\varepsilon(\omega) = \varepsilon_1(\omega) + i\varepsilon_2(\omega)$$

The imaginary part is investigated based on the Fermi distribution and the crystal wave function [25,26]:

$$\varepsilon_2(\omega) = \frac{4\pi^2 e^2}{\Omega m^2 \omega^2} \sum_{knn'\sigma} \langle k, n, \sigma, |p_i|, k, n' \rangle \sigma \times \langle k, n', \sigma, |p_i|, k, n, \sigma \rangle k_{kn} (1 - f_{kn'}) \delta(e_{kn'} - e_{kn} - \hbar\omega)$$

Table 1. Band gap energy, lattice constants, and bond lengths of Mo_2CF_2, $Mo_2C(OH)_2$, and Mo_2CO_2.

	MXenes	Gap (eV)	a = b (Å)	c (Å)	d_{Mo-C} (Å)	$d_{Mo-(F, O, H)}$ (Å)
Monolayer	Mo_2CF_2	0.278	3.2786	35.7215	2.1148	2.3029
	$Mo_2C(OH)_2$	0.117	3.3012	36.2148	2.1264	2.9868
	Mo_2CO_2	-	2.8836	30.0007	2.1608	2.0678
Bilayer	Mo_2CF_2	0.258	3.2793	35.7128	2.1151	2.3032
	$Mo_2C(OH)_2$	0.012	3.3013	36.2149	2.1264	2.9868
	Mo_2CO_2	-	2.8837	30.0008	2.1609	2.0678
Trilayer	Mo_2CF_2	0.249	3.2798	35.7058	2.1154	2.3036
	$Mo_2C(OH)_2$	-	3.3013	36.2149	2.1264	2.9868
	Mo_2CO_2	-	2.8837	30.0008	2.1609	2.0678

Here e, m, and Ω are the electron charge, mass, and crystal volume, respectively. The crystal wave function $|kn\sigma>$ is proportional to the eigenvalue nth, the crystal momentum k, and the spin σ. By using the Kramers–Kronig transformation [27–29], the real part $\varepsilon_1(\omega)$ can be extracted from the imaginary part $\varepsilon_2(\omega)$. Once the dielectric function $\varepsilon(\omega)$ has been determined, based on the standard optical relationships, all other optical parameters, such as the refractivity, reflectivity, and absorption or optical conductivity, can be estimated.

The Boltzmann's transport equation (BTE) within the constant relaxation time (τ) approximation is employed for calculating the thermoelectric (TE) properties of Mo_2C-MXenes based on the electronic structure results. The BoltzTrap code is a well-established computational simulation tool for TE properties [30]. The dimensionless figure of merit (ZT) describes the TE performance of a material, and is given as:

$$ZT = \frac{S^2\sigma}{\kappa}T$$

where S is the Seebeck coefficient; σ is the electrical conductivity; κ is the thermal conductivity; and T is the absolute temperature [31].

It should be noted that the ideal TE material is defined as having a high ZT value, in which the specifications include a high power factor with a high Seebeck coefficient (S), high electrical conductivity (σ), and low thermal conductivity (κ). On the other hand, these quantities depend on τ and are difficult to track down solely through band structure analysis. However, all investigated Mo_2C- have the same hexagonal structure, and they initially all belong to the same material family as MAX phases. Therefore, the electron-scattering mechanisms in Mo_2C- can be predicted to be similar, and the comparison of thermoelectric results is meaningful. The calculation results of the thermoelectric properties are presented and compared at different temperatures in the range of 300–600 K for all monolayer and multilayer structures.

3. Results and Discussion

3.1. Crystal Structure

Figure 1 illustrates the structure of monolayer and multilayer Mo_2C-materials with different functional groups. These materials have a structure consisting of Mo atoms located in the outer layers, sandwiching the layers of C and two layers of Mo atoms halogenated by atomic layers -F, -OH, and -O on each side, thus creating a similar surface chemistry. In comparison, all MXenes with surface functional groups are more stable than bare MXenes [11].

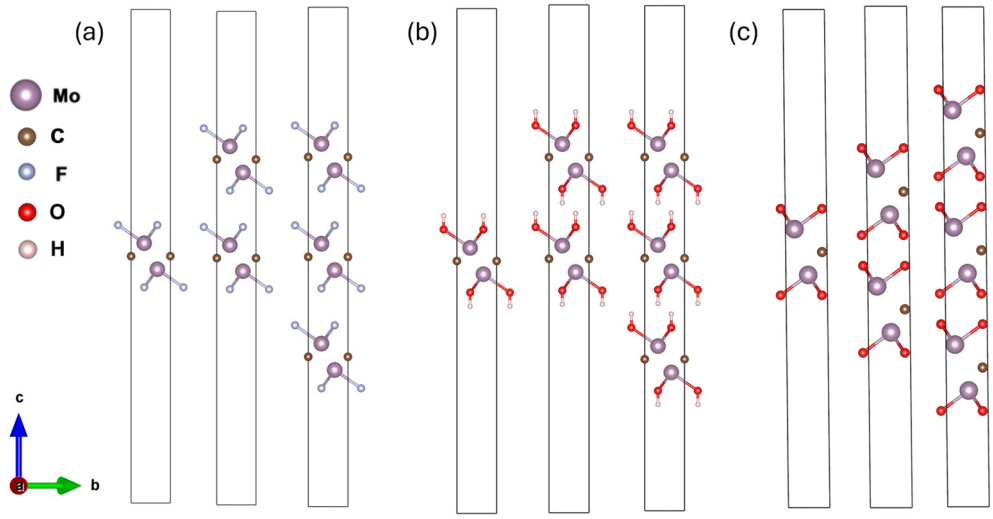

Figure 1. Structure of monolayer and multilayer for Mo_2CF_2 (**a**), $Mo_2C(OH)_2$ (**b**), and Mo_2CO_2 (**c**) MXenes.

The lattice constants and bond lengths of Mo_2CF_2, $Mo_2C(OH)_2$, and Mo_2CO_2 are summarized in Table 1. It should be noted that these parameters were nearly the same for each structure because the number of layers increased while the lattice parameter along the c axis remained unchanged. The results of structural optimization for Mo_2CF_2 are similar to the previous report [32], with a difference of only less than 1 because the same simulation package and pseudopotential were used. Experimental results on the band gap energy, lattice constant, and bond length of different Mo_2C-MXenes are still lacking.

3.2. Electronic Properties

Figure 2 show the energy band structures of monolayer and multilayer Mo_2CF_2, $Mo_2C(OH)_2$, and Mo_2CO_2. Monolayer Mo_2CF_2 and $Mo_2C(OH)_2$ are semiconductor materials with indirect band gap energies of 0.278 eV and 0.117 eV, respectively. Meanwhile, monolayer Mo_2CO_2 behaves like a metal, with no band gap energy. The peaks in the valence bands of Mo_2CF_2 and $Mo_2C(OH)_2$ were shifted to zero energy. The valence band maximum and conduction band minimum of these materials were located at the k point between K and G. Our calculations of the band gap energies for monolayer Mo_2CF_2 and $Mo_2C(OH)_2$ are similar to the previously reported 0.25 eV and 0.11 eV, respectively, which were also calculated using the GGA-PBE function [23,32]. The calculation results indicate that the band gap energy changed depending on the surface functional group.

Like the monolayer Mo_2C-, the energy band structures of multilayer Mo_2C-MXenes showed similar band shapes, especially for the valence and conduction bands of each material. Bilayer and trilayer Mo_2CF_2 still exhibited semiconductor properties with band gap energy values of 0.258 eV and 0.249 eV, respectively. A semiconducting-to-metallic behavior was observed in the multilayer $Mo_2C(OH)_2$ MXenes when increasing the number of layers of the material. The bandgap changed from about 0.012 eV for the bilayer to 0 eV (no bandgap) for the trilayer $Mo_2C(OH)_2$. Our results show a reversal to the band gap energy as the number of layers increased. The band gap energy reduction was related to the coupling between layers, leading to the splitting of the bands [32]. The band splitting had a high dependence on the number of layers. As can be seen in Figure 2, the interlayer coupling was stronger from the monolayer to the trilayer, leading to an increase in the band splitting and a decrease in the band gap energy. This indicates that the band gap of 2D layered Mo_2C- can be tuned by engineering the number of layers and enhancing this characteristic for electronic device applications. Mo_2CO_2 still exhibited a metallic behavior in both the bilayer and trilayer structures.

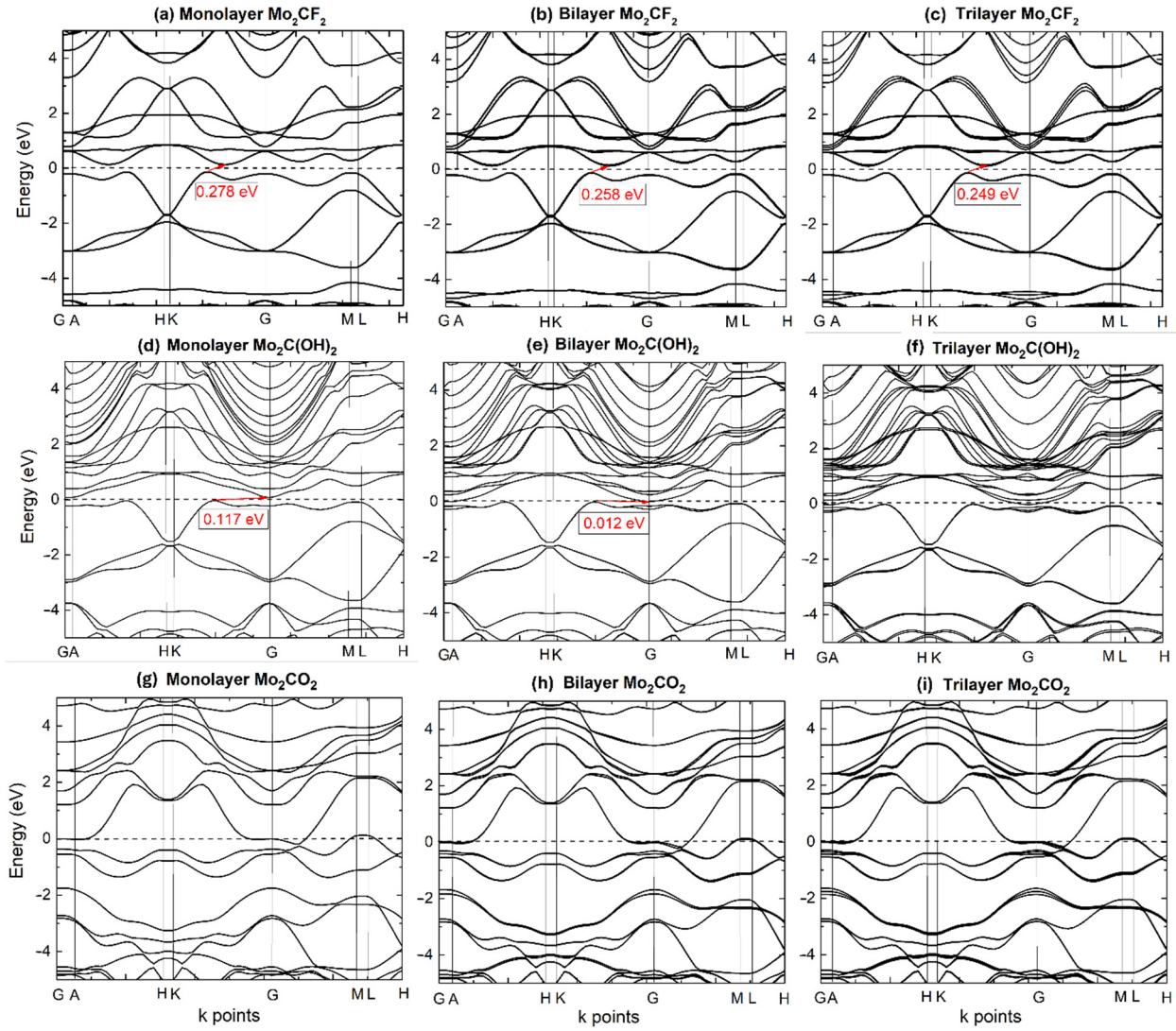

Figure 2. Electronic band structures of monolayer and multilayer for Mo_2CF_2, $Mo_2C(OH)_2$, and Mo_2CO_2 MXenes.

The semiconducting or metallic state transition comes from the electron counting rule between the dangling bond states and the additional states created at the Fermi level [33]. Typically, the transition metal d-electrons play an important role in the DOS near the Fermi surface, whereas the p-electrons of the C atoms are composed below the Fermi surface. Additionally, the electronic properties are mainly impacted by the surface terminations bonded to the outer transition metal layers [34,35]. Therefore, a similar effect could be seen in the surface terminal groups OH- and F-, which accept for only one electron, whereas the O= group receives two electrons from the outer metal layers, representing a different effect. This effect suggests that a new energy band can be formed below the Fermi surface, which can spontaneously reduce the DOS at the Fermi surface (see Figure 3).

3.3. Optical Properties

The real part $\varepsilon_1(\omega)$ and the imaginary part $\varepsilon_2(\omega)$ of the dielectric function for Mo_2CF_2, $Mo_2C(OH)_2$, and Mo_2CO_2 with different layers are presented in Figure 4. The calculated values of $\varepsilon_1(0)$ were 5.76, 7.65, and 10.60 for the Mo_2CF_2, $Mo_2C(OH)_2$, and Mo_2CO_2 monolayers, respectively. Our calculation results for the real part $\varepsilon_1(\omega)$ of all Mo_2C-structures show that, from 0 to 6 eV, the intensity of the peaks increased with the increasing number of layers. The maximum value of $\varepsilon_1(\omega)$ was achieved at about 0.67 eV, 0.21 eV, and

1.48 eV for the 2D sublayers of Mo_2CF_2, $Mo_2C(OH)_2$, and Mo_2CO_2, respectively. Obtaining higher values of $\varepsilon_1(\omega)$ indicated a large polarizability of the incident photon energy as the number of layers increased. The higher value of $\varepsilon_1(\omega)$ for Mo_2CO_2 showed the greater polarization ability of the -O functional groups compared to -F, -OH. In particular, when moving toward higher incident photon energies, we observed inflection point positions, where $\varepsilon_1(\omega)$ began to take negative values. One inflection point was observed for the Mo_2CF_2 material at about 6 eV, while two inflection points were observed for $Mo_2C(OH)_2$ at 1.28 eV and 4.76 eV and for Mo_2CO_2 at 1.78 eV and 4.15 eV. We found that increasing the number of layers led to the magnitude of the $\varepsilon_1(\omega)$ peaks decreasing and becoming more negative starting at these inflection point values.

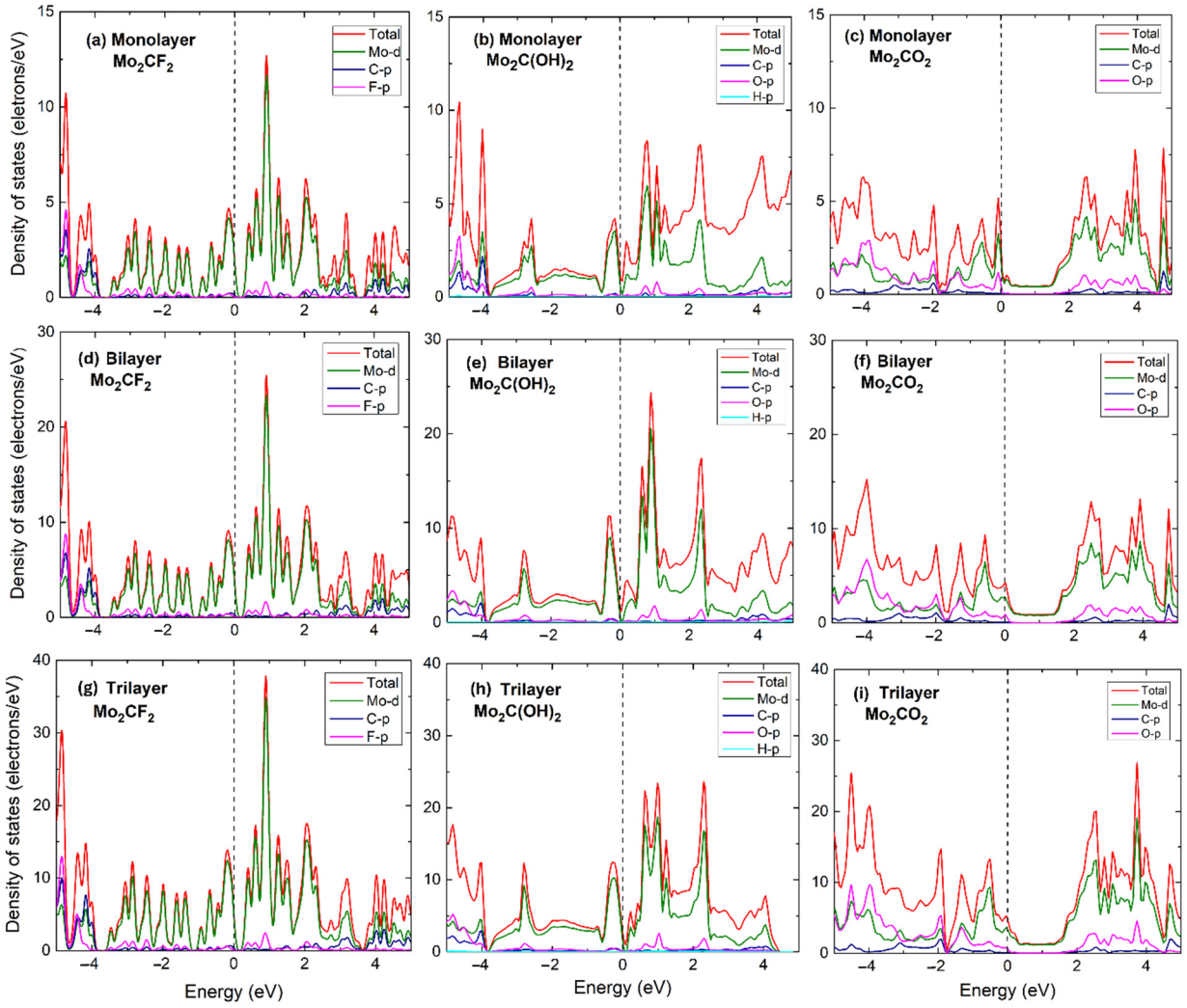

Figure 3. Total and partial density of states for 2D layered Mo_2CF_2, $Mo_2C(OH)_2$ and Mo_2CO_2.

The dependences of the imaginary part of the dielectric function $\varepsilon_2(\omega)$ on the number of Mo_2C-MXene layers is also shown in Figure 4, whereby increasing the Mo_2C-MXenes layers led to an increase in the intensity of $\varepsilon_2(\omega)$. The electronic band structure of Mo_2C-, especially the transition between the valence band and the conduction band, is related to the imaginary component. Therefore, the optical band gap energy of the 2D Mo_2C-sublayer can be estimated from $\varepsilon_2(\omega)$. Above the optical bandgap energy, we obtained a sharp increase in the intensity of $\varepsilon_2(\omega)$, with its maximum occurring at 1.12 eV and 0.78 eV for Mo_2CF_2 and $Mo_2C(OH)_2$, respectively. These results show that Mo_2CO_2 had a relatively large visible-light absorption area under the $\varepsilon_2(\omega)$ curve. In the photon energy interval 1.5–3 eV, the intensity of $\varepsilon_2(\omega)$ increased, with its peak occurring at 1.88 eV for

both layers of Mo_2CO_2. The electron transition between the Mo-4d state to the Mo-5d state was attributed to the peak, as represented in the density of states of Mo_2CF_2, $Mo_2C(OH)_2$, and Mo_2CO_2 (see Figure 3). It was found that the =O functional group of Mo_2C- had a larger absorption coefficient than the -F and -OH terminated ones, making them suitable for applications in the field of transparent electrodes [36]. These findings suggest that the optical characteristics of the 2D layered Mo_2C- can be engineered by the functional groups and the number of layers [37].

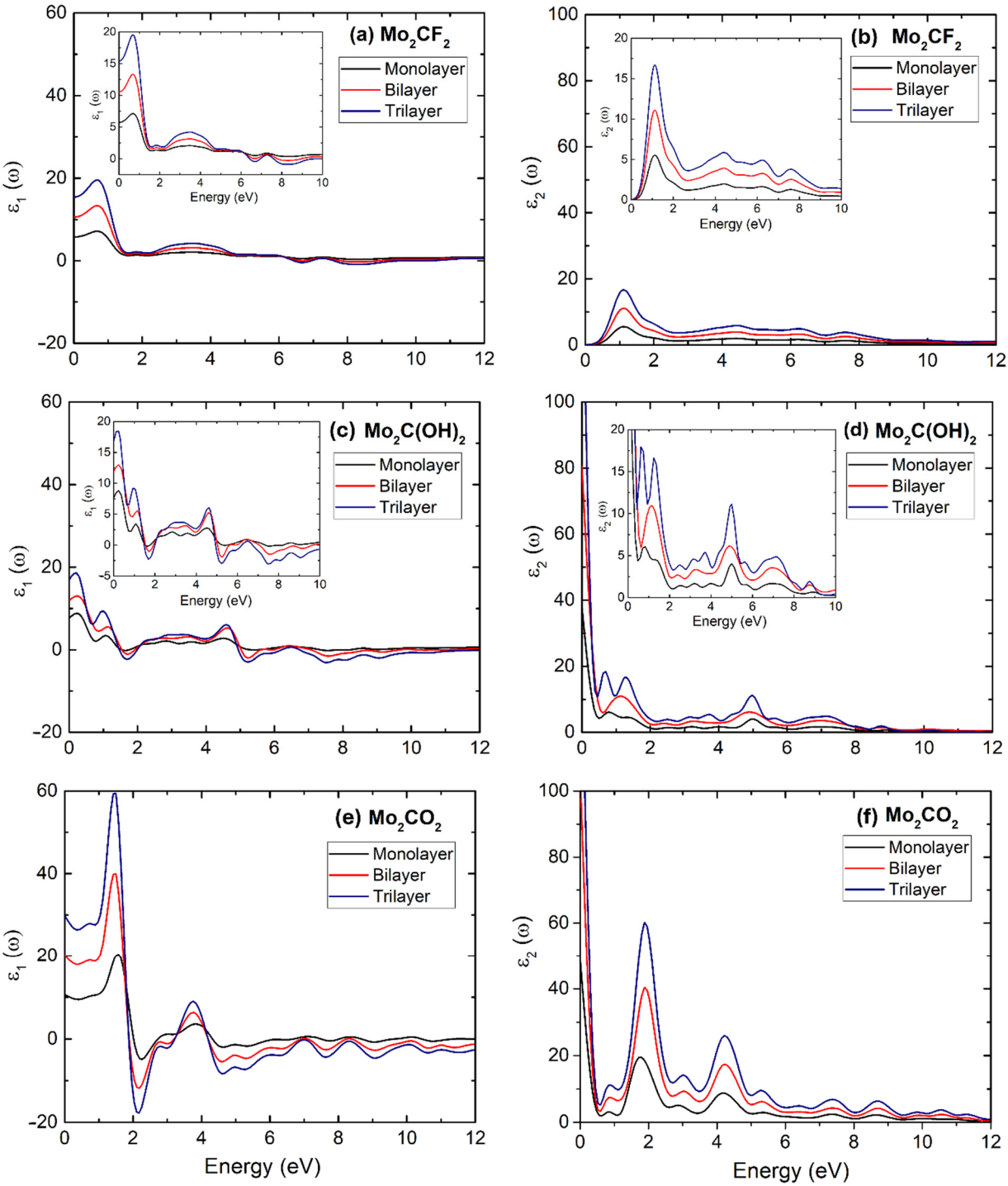

Figure 4. Real part and imaginary part of the dielectric function of monolayer and multilayer for Mo_2CF_2, $Mo_2C(OH)_2$, and Mo_2CO_2.

3.4. Thermoelectric Properties

In this section, the thermoelectric properties of monolayer and multilayer Mo_2C- are investigated because their structure has been shown to have good mobility [23]. In general, at high temperatures and low chemical potential, charge carriers reduce the Seebeck coefficient and the electrical conductivity and increase the thermal conductivity of the Mo_2CF_2 and $Mo_2C(OH)_2$ semiconductors. The Seebeck coefficient S, calculated at different temperatures as a function of the chemical potential, is shown in Figure 5. The results show that at room temperature, monolayer $Mo_2C(OH)_2$ and Mo_2CF_2 attained high Seebeck coefficients of about 285 μV K^{-1} and 400 μV K^{-1}, respectively. This indicates that, with the large transition of the DOS, large Seebeck coefficient values can be obtained. Particularly, an interesting transition from p-type to n-type is shown for the Mo_2CF_2 and $Mo_2C(OH)_2$ semiconductors, representing the chemical potential transition from a low carrier concentration to a high concentration. The calculation results for the Seebeck coefficient of Mo_2CO_2 showed a drastic transition, especially at room temperature.

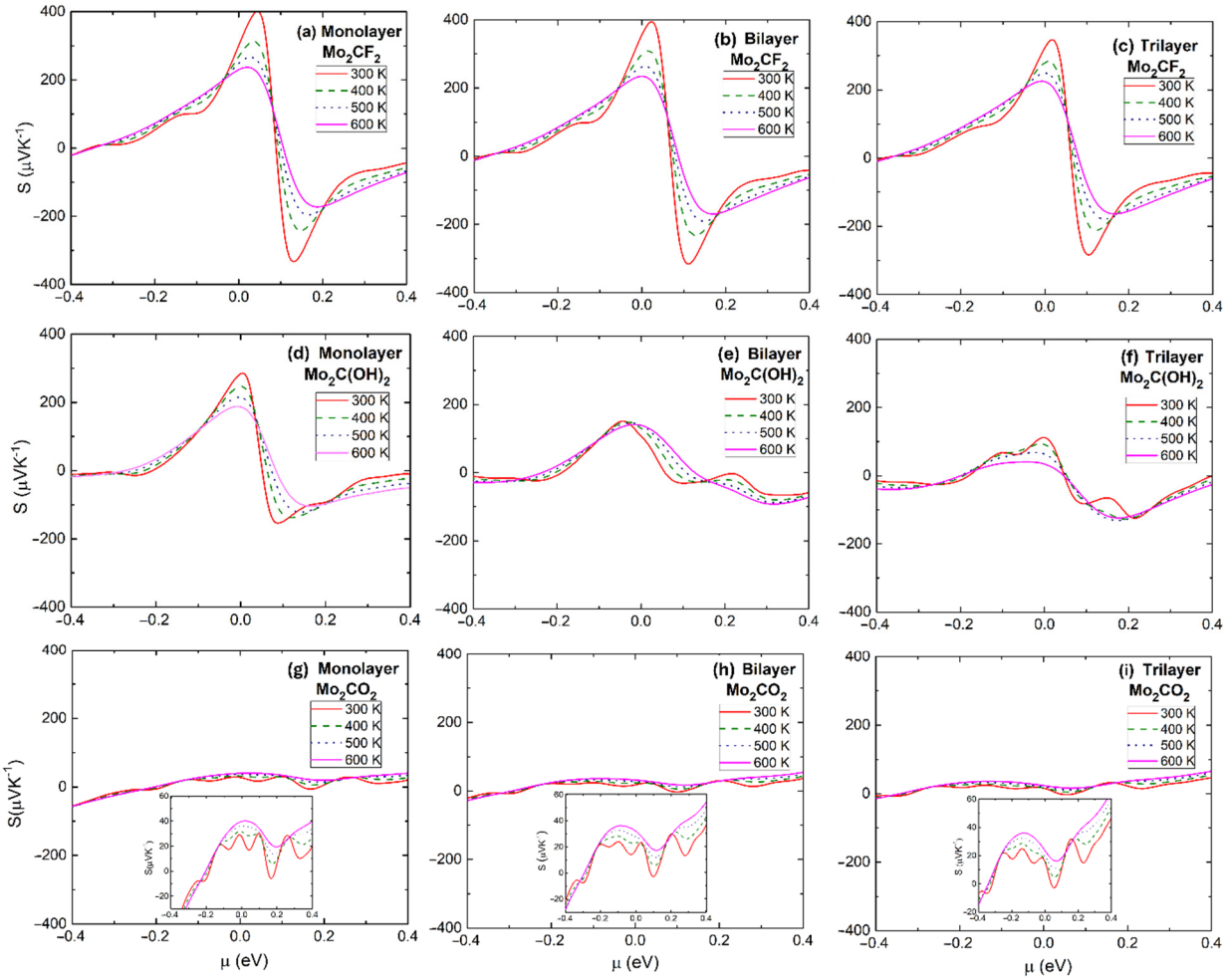

Figure 5. Seebeck coefficient as a function of the chemical potential for monolayer and multilayer at different temperatures for Mo_2CF_2, $Mo_2C(OH)_2$, and Mo_2CO_2.

Bilayer Mo_2CF_2 with a band gap of 0.258 eV still exhibited a large Seebeck coefficient (~395 μVK^{-1}) and a relatively high conductivity (~9 × 10^{19} Ω^{-1} cm^{-1} s^{-1}) at low carrier concentrations, and, therefore, a high power factor. $Mo_2C(OH)_2$ had a smaller band gap (0.012 eV) with a smaller Seebeck coefficient compared to Mo_2CF_2 (~150 μVK^{-1}), as well as a small electrical conductivity near its band edges. Meanwhile, Mo_2CO_2 was still metallic and did not exhibit better TE properties. The calculations demonstrate that Mo_2CF_2 and $Mo_2C(OH)_2$ can be promising TE materials in the low- and intermediate-temperature

regions. This is consistent with theoretical predictions [23], which found that Mo_2CF_2 nanosheets achieved larger power factors compared to other functionalized MXenes.

Figure 6 shows the electrical conductivity of Mo_2C-structures as a function of chemical potential at different temperatures. From −0.4 to −0.1 eV, the electrical conductivity decreased as the temperature increased from 300 K to 600 K. The monolayer Mo_2CF_2 obtained the maximum electrical conductivity value at around −0.3 eV. Moving towards higher chemical potential values, the observed temperature-dependent electrical conductivity was reversible at around −0.15 eV for Mo_2CF_2 and $Mo_2C(OH)_2$ and −0.1 eV for the monolayer Mo_2CO_2, in which the electrical conductivity increased as the temperature increased.

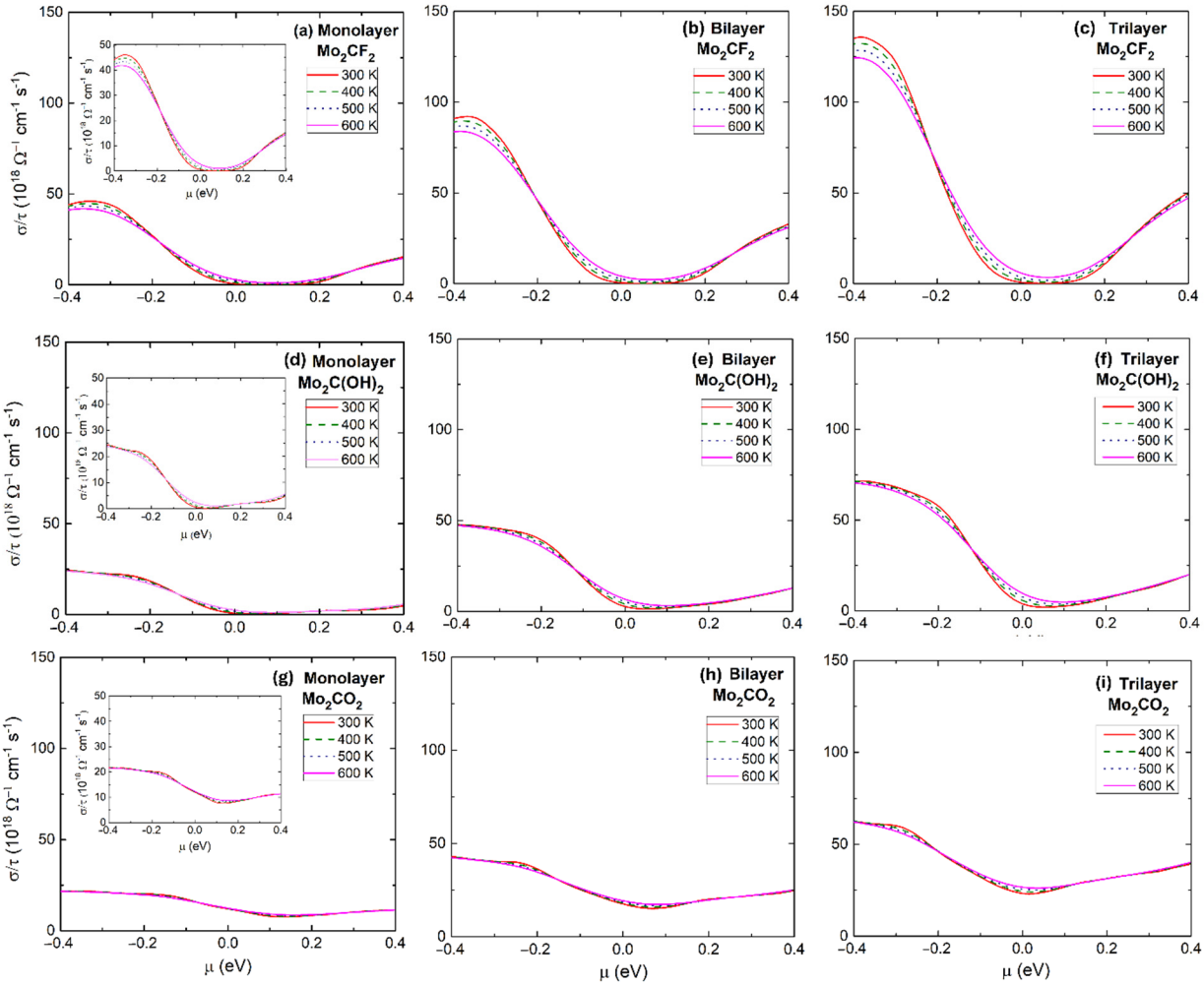

Figure 6. Electrical conductivity as a function of the chemical potential at different temperatures from 300 K to 600 K for monolayer and multilayer Mo_2CF_2, $Mo_2C(OH)_2$, and Mo_2CO_2, respectively.

The calculation results of electronic thermal conductivity as a function of chemical potential at different temperatures are presented in Figure 7. For the electronic thermal conductivity, a similar trend was observed for all three Mo_2C-MXenes. At small chemical potential values or at high temperature values, the electronic thermal conductivity was higher, tended to be steeper, and gradually decreased to a minimum value at an energy level equal to the Fermi level. Unlike the rapid change detailed above, the dependence of thermal conductivity on temperature at large chemical potential values underwent a slow change. At room temperature, Mo_2CF_2 and $Mo_2C(OH)_2$ exhibited a low electronic thermal conductivity of 0 W m^{-1} K^{-1} s^{-1} at the Fermi level, while this value was around 10 W m^{-1} K^{-1} s^{-1} for Mo_2CO_2 at the same position. This is consistent with the classical description that when the carrier density is small, the electronic thermal conductivity must

be small. Particularly, the electronic and thermal transport [38,39] can be attributed to the surface functional groups in MXenes, in which -F and -OH terminated showed the largest electronic transmission compared to =O terminated MXenes.

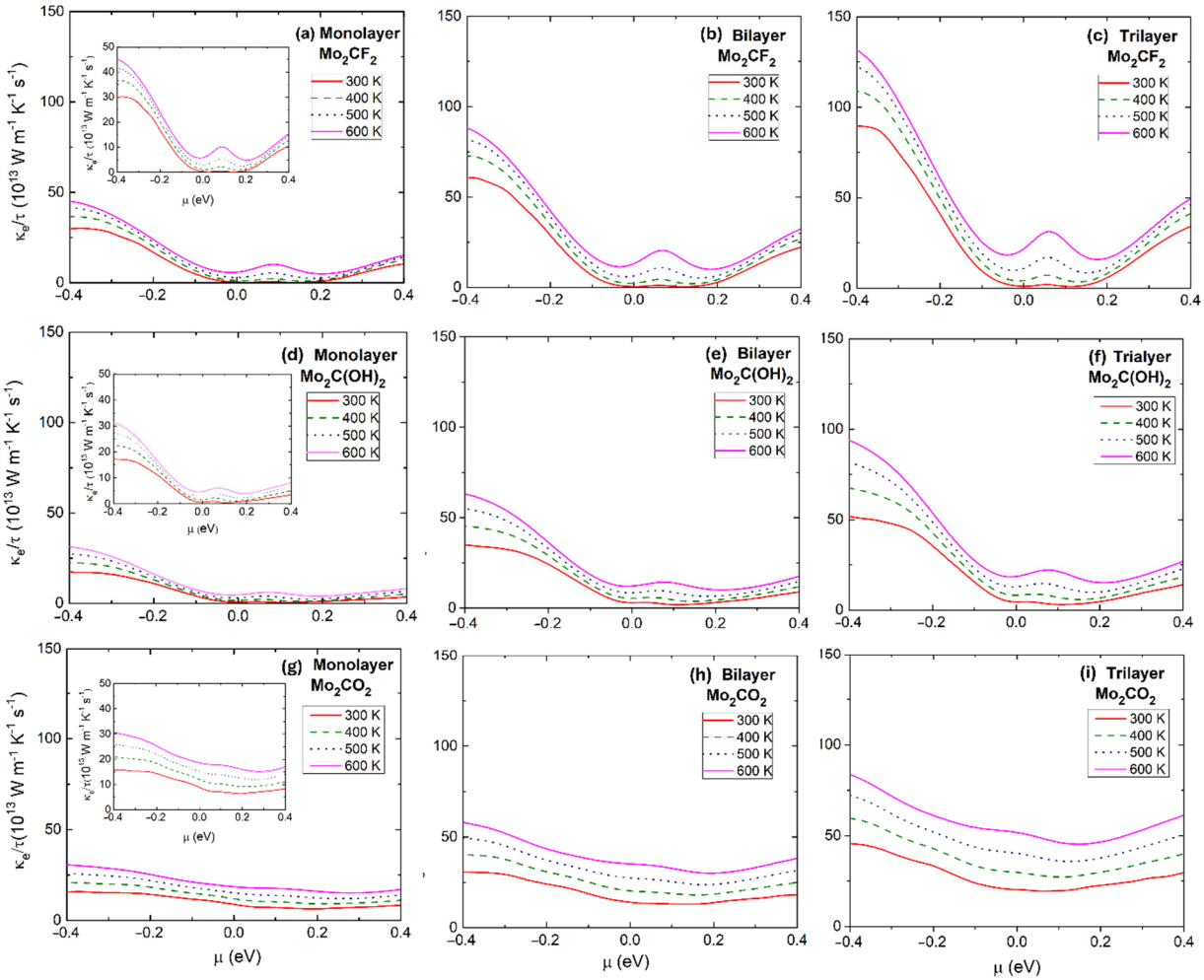

Figure 7. Electronic thermal conductivity of Mo_2CF_2, $Mo_2C(OH)_2$, and Mo_2CO_2 monolayer and multilayer structures as a function of chemical potential at different temperatures from 300–600 K.

Overall, the results show that there was no significant difference between the monolayer structures and their corresponding multilayer structures in terms of electronic and thermoelectric properties. This indicates that the interlayer interactions in Mo_2C-multilayers are relatively weak. Like the trend observed for electronic structure of Mo_2CF_2 and $Mo_2C(OH)_2$ from monolayer to multilayer, where increasing the number of Mo_2C-layers led to a narrower band gap energy, the value of the Seebeck coefficient also decreased as a function of the number of layers. The electrical conductivity and electronic thermal conductivity of all Mo_2C-structure when the number of Mo_2C-layers was increased. The electrical conductivity and thermal conductivity of Mo_2CF_2 were higher than those of $Mo_2C(OH)_2$ due to its special energy band structure. As can be seen in Figure 2, the energy bands below the valence band maximum were relatively flat, but there was a part from the A–H midpoint to the K–G midpoint that was linearly dispersed. Such a band structure can create a relatively large Fermi surface and Fermi velocity, and is desirable for high-performance thermoelectric devices. Based on such special band shapes, a general rule for the design of high-performance thermoelectric materials is proposed as follows: When the Fermi level is near the energy boundaries, a combination of relatively flat and relatively dispersed parts in the band structure can create a large Seebeck coefficient, a low resistivity, and, thus, a

large thermal coefficient. It should be noted that it is not possible to directly compare the electrical conductivity and electronic thermal conductivity of monolayers with multilayers because these quantities depend on volume, and it is not possible to accurately determine the thickness of the monolayer.

4. Conclusions

Using electronic structure calculations based on Density Functional Theory and Boltzmann transport theory, we investigated the electronic, optical, and thermoelectric properties of the Mo_2CF_2, $Mo_2C(OH)_2$, and Mo_2CO_2 MXenes from their respective monolayers to multilayers. Our results show that Mo_2CF_2 and $Mo_2C(OH)_2$ are semiconductors with indirect band gap energies of 0.278 eV and 0.117 eV for the monolayers Mo_2CF_2 and $Mo_2C(OH)_2$, respectively. On the other hand, Mo_2CO_2 behaves like a metal with no band gap energy. Increasing the number of layers results in narrower band gap energy of the 2D layered Mo_2CF_2 and $Mo_2C(OH)_2$ due to interlayer coupling. The band gap energy of the bilayer Mo_2CF_2 and $Mo_2C(OH)_2$ are 0.258 eV and 0.012 eV, respectively. These results indicate that the band gap energy of the Mo_2C-material can be adjusted by the number of layers.

For the optical properties of Mo_2C-sublayers affected by different -F, -OH, and -O functional groups, a higher value of dielectric function was obtained for Mo_2CO_2 compared to Mo_2CF_2 and $Mo_2C(OH)_2$ ($\varepsilon_1(\omega)$ ~60 at around 1.48 eV for the trilayer Mo_2CO_2), indicating a greater polarizability and visible light absorption. Controlling the band gap energy can manipulate the dielectric constant and optical properties of 2D layered Mo_2CF_2 and $Mo_2C(OH)_2$. This ability makes Mo_2C- a promising material for applications in the field of electronics.

Regarding thermoelectric properties, Mo_2CF_2 showed the best thermoelectric properties among the three types of Mo_2C-MXenes considered in this study. The remarkable thermoelectric properties of Mo_2CF_2 are a result of its semiconductor band gap and special band shape near the energy boundaries, which has potential for high-performance thermoelectric devices.

Opportunities and challenges for Mo_2C-MXene application coexist, and future efforts should pay more attention to the synthesis and study of other MXenes containing Mo, V, Zr, etc. There is a lack of experimental studies on these materials with different numbers of layers. Therefore, it would be ideal to further study the preparation method of MXenes and combine computational calculations with experiments to enhance the predictions of the characteristics and the properties of these materials. Currently, with the fabrication of materials that control thickness according to the number of layers, research results regarding flexible bandgap energy and high-temperature thermal stability demonstrate the potential of Mo_2C-MXene for many applications, including energy storage, solar cells, and electrode applications, by optimizing the thin film layer.

Author Contributions: Methodology and validation, M.C.-R. and L.V.M.; formal analysis and investigation, D.T.K.A.; writing—original draft preparation, D.T.K.A. and D.M.H.; writing—review and editing, P.H.M., K.Y., M.C.-R., L.V.M. and N.D.H.; funding acquisition, P.H.M. and M.C.-R.; supervision, P.H.M. All authors have read and agreed to the published version of the manuscript.

Funding: This work is supported by Vietnam Academy of Science and Technology through Project No. NVCC05.03/24-25 and the Osaka University, Institute of Laser Engineering Collaborative Research Fund (2024B1-008).

Institutional Review Board Statement: Not applicable.

Informed Consent Statement: Not applicable.

Data Availability Statement: The data that support the findings of this study are available from the corresponding author upon reasonable request.

Conflicts of Interest: On behalf of all authors, the corresponding author states that there are no conflicts of interest.

References

1. Novoselov, K.S.; Geim, A.K.; Morozov, S.V.; Jiang, D.; Zhang, Y.; Dubonos, S.V.; Grigorieva, I.V.; Firsov, A.A. Electric field effect in atomically thin carbon films. *Science* **2004**, *306*, 666–669. [CrossRef]
2. Geim, A.K.; Novoselov, K.S. The rise of graphene. In *Nanoscience and Technology: A Collection of Reviews from Nature Journals*; World Scientific: Singapore, 2010; pp. 11–19.
3. Choi, W.; Choudhary, N.; Han, G.H.; Park, J.; Akinwande, D.; Lee, Y.H. Recent development of two-dimensional transition metal dichalcogenides and their applications. *Mater. Today* **2017**, *20*, 116–130. [CrossRef]
4. Yang, L.; Chen, W.; Yu, Q.; Liu, B. Mass production of two-dimensional materials beyond graphene and their applications. *Nano Res.* **2021**, *14*, 1583–1597. [CrossRef]
5. Naguib, M.; Kurtoglu, M.; Presser, V.; Lu, J.; Niu, J.; Heon, M.; Hultman, L.; Gogotsi, Y.; Barsoum, M.W. Two-dimensional nanocrystals produced by exfoliation of Ti_3AlC_2. *Adv. Mater.* **2011**, *23*, 4248–4253. [CrossRef]
6. Li, F.; Jiang, J.; Wang, J.; Zou, J.; Sun, W.; Wang, H.; Xiang, K.; Wu, P.; Hsu, J.P. Porous 3D carbon-based materials: An emerging platform for efficient hydrogen production. *Nano Res.* **2022**, *16*, 127–145. [CrossRef]
7. Naguib, M.; Come, J.; Dyatkin, B.; Presser, V.; Taberna, P.L.; Simon, P.; Barsoum, M.W.; Gogotsi, Y. MXene: A promising transition metal carbide anode for lithium-ion batteries. *Electrochem. Commun.* **2012**, *16*, 61–64. [CrossRef]
8. Naguib, M.; Barsoum, M.W.; Gogotsi, Y. Ten years of progress in the synthesis and development of MXenes. *Adv. Mater.* **2021**, *33*, 2103393. [CrossRef]
9. Cakır, D.; Sevik, C.; Gulseren, O.; Peeters, F.M. Mo_2C as a high capacity anode material: A first-principles study. *J. Mater. Chem. A* **2016**, *4*, 6029–6035. [CrossRef]
10. Fredrickson, K.D.; Anasori, B.; Seh, Z.W.; Gogotsi, Y.; Vojvodic, A. Effects of applied potential and water intercalation on the surface chemistry of Ti_2C and Mo_2C MXenes. *J. Phys. Chem. C* **2016**, *120*, 28432–28440. [CrossRef]
11. Anasori, B.; Lukatskaya, M.R.; Gogotsi, Y. 2D metal carbides and nitrides (MXenes) for energy storage. *Nat. Rev. Mater.* **2017**, *2*, 16098. [CrossRef]
12. Frey, N.C.; Wang, J.; Vega Bellido, G.I.; Anasori, B.; Gogotsi, Y.; Shenoy, V.B. Prediction of synthesis of 2D metal carbides and nitrides (MXenes) and their precursors with positive and unlabeled machine learning. *ACS Nano* **2019**, *13*, 3031–3041. [CrossRef] [PubMed]
13. Pan, J.; Lany, S.; Qi, Y. Computationally driven two-dimensional materials design: What is next? *ACS Nano* **2017**, *11*, 7560–7564. [CrossRef] [PubMed]
14. Zhang, X.; Liu, Y.; Dong, S.; Yang, J.; Liu, X. Flexible electrode based on multi-scaled MXene ($Ti_3C_2T_x$) for supercapacitors. *J. Alloys Compd.* **2019**, *790*, 517–523. [CrossRef]
15. Xiao, J.; Wen, J.; Zhao, J.; Ma, X.; Gao, H.; Zhang, X. A safe etching route to synthesize highly crystalline Nb_2CT_x MXene for high performance asymmetric supercapacitor applications. *Electrochim. Acta.* **2020**, *337*, 135803. [CrossRef]
16. Meshkian, R.; Ake Naslund, L.; Halim, J.; Lu, J.; Barsoum, M.W.; Rosen, J. Synthesis of two-dimensional molybdenum carbide, Mo_2C, from the gallium based atomic laminate Mo_2Ga_2C. *Scr. Mater.* **2015**, *108*, 147–150. [CrossRef]
17. Hu, C.; Lai, C.C.; Tao, Q.; Lu, J.; Halim, J.; Sun, L.; Zhang, J.; Yang, J.; Anasori, B.; Wang, J.; et al. Mo_2Ga_2C: A new ternary nanolaminated carbide. *Chem. Commun.* **2015**, *51*, 6560–6563. [CrossRef]
18. Yorulmaz, U.; Demiroglu, I.; Cakir, D.; Gulseren, O.; Sevik, C. A systematical ab-initio review of promising 2D MXene monolayers towards Li-ion battery applications. *J. Phys. Energy* **2020**, *2*, 032006. [CrossRef]
19. Seh, Z.W.; Fredrickson, K.D.; Anasori, B.; Kibsgaard, J.; Strickler, A.L.; Lukatskaya, M.R.; Gogotsi, Y.; Jaramillo, T.F.; Vojvodic, A. Two-dimensional molybdenum carbide (MXene) as an efficient electrocatalyst for hydrogen evolution. *ACS Energy Lett.* **2016**, *1*, 589–594. [CrossRef]
20. Jin, S.; Jing, H.J.; Wang, L.B.; Hu, Q.; Zhou, A. Construction and performance of CdS/MoO_2@Mo_2C-MXene photocatalyst for H_2 production. *J. Adv. Ceram.* **2022**, *11*, 1431–1444. [CrossRef]
21. Jin, S.; Wu, J.B.; Jiang, J.Z.; Wang, R.; Zhou, B.; Wang, L.; Hua, Q.; Zhou, A. Boosting photocatalytic performance of $Cd_xZn_{1-x}S$ for H_2 production by Mo_2C MXene with large interlayer distance. *J. Mater. Chem. A* **2023**, *11*, 5851–5863. [CrossRef]
22. Liu, X.; Xu, H.; Xie, F.; Fasel, C.; Yin, X.; Riedel, R. Highly flexible and ultrathin Mo_2C film via in-situ growth on graphene oxide for electromagnetic shielding application. *Carbon* **2020**, *163*, 254–264. [CrossRef]
23. Khazaei, M.; Arai, M.; Sasaki, T.; Estilic, M.; Sakka, Y. Two-dimensional molybdenum carbides: Potential thermoelectric materials of the MXene family. *Phys. Chem. Chem. Phys.* **2014**, *16*, 7841. [CrossRef]
24. Kresse, G.; Marsman, M.; Furthmuller, J. *Vienna Ab initio Simulation Package (VASP), The Guide*; Computational Materials Physics; Faculty of Physics, Universität Wien: Vienna, Austria, 2014.
25. Lashgari, H.; Abolhassani, M.R.; Boochani, A.; Elahi, S.M.; Khodadadi, J. Electronic and optical properties of 2D graphene-like compounds titanium carbides and nitrides: DFT calculations. *Solid State Commun.* **2014**, *195*, 61–69. [CrossRef]
26. Bai, Y.; Zhou, K.; Srikanth, N.; Pang, J.H.L.; He, X.; Wang, R. Dependence of elastic and optical properties on surface terminated groups in two-dimensional MXene monolayers: A first-principles study. *RSC Adv.* **2016**, *6*, 35731–35739. [CrossRef]
27. Hutchings, D.C.; Sheik-Bahae, M.; Hagan, D.J.; Van Stryland, E.W. Kramers-Krönig relations in nonlinear optics. *Opt. Quantum Electron.* **1992**, *24*, 1–30. [CrossRef]
28. Kronig, R.D.L. On the theory of dispersion of X-rays. *J. Opt. Soc. Am.* **1926**, *12*, 547–557. [CrossRef]

29. Kramers, H.A. La diffusion de la lumiere par les atomes. *Atti Cong. Intern. Fisica (Trans. Volta Centen. Congr.) Como* **1927**, *2*, 545–557. Available online: https://cir.nii.ac.jp/crid/1571135649980336384 (accessed on 10 September 2024).
30. Madsen, G.K.; Singh, D.J. BoltzTraP. A code for calculating band-structure dependent quantities. *Comput. Phys. Commun.* **2006**, *175*, 67. [CrossRef]
31. Tritt, T.M.; Subramanian, M.A. Thermoelectric Materials, Phenomena, and Applications: A Bird's Eye View. *MRS Bull.* **2006**, *31*, 188–198. [CrossRef]
32. Anh, D.T.K.; Mui, L.V.; Minh, P.H.; Binh, N.T.; Cadatal-Raduban, M. Engineering the band gap and optical properties of a two-dimensional molybdenum carbon fluoride MXene. *Acta Crystallogr. B* **2022**, *78*, 5. [CrossRef]
33. Khazaei, M.; Arai, M.; Sasaki, T.; Chung, C.Y.; Venkataramanan, N.S.; Estili, M.; Sakka, Y.; Kawazoe, Y. Novel electronic and magnetic properties of two-dimensional transition metal carbides and nitrides. *Adv. Funct. Mater.* **2013**, *23*, 2185–2192. [CrossRef]
34. Anasori, B.; Xie, Y.; Beidaghi, M.; Lu, J.; Hosler, B.C.; Hultman, L.; Kent, P.R.C.; Gogotsi, Y.; Barsoum, M.W. Two-dimensional, ordered, double transition metals carbides (MXenes). *ACS Nano* **2015**, *9*, 9507–9516. [CrossRef] [PubMed]
35. Dong, L.; Kumar, H.; Anasori, B.; Gogotsi, Y.; Shenoy, V.B. Rational design of two-dimensional metallic and semiconducting spintronic materials based on ordered double-transition-metal MXenes. *J. Phys. Chem. Lett.* **2017**, *8*, 422–428. [CrossRef]
36. Berdiyorov, G.R. Optical properties of functionalized $Ti_3C_2T_2$ (T = F, O, OH) MXene: First-principles calculations. *AIP Adv.* **2016**, *6*, 055105. [CrossRef]
37. Hart, J.L.; Hantanasirisakul, K.; Lang, A.C.; Anasori, B.; Pinto, D.; Pivak, Y.; Van Omme, J.T.; May, S.J.; Gogotsi, Y.; Taheri, M.L. Control of MXenes' electronic properties through termination and intercalation. *Nature Commun.* **2019**, *10*, 522. [CrossRef] [PubMed]
38. Berdiyorov, G.R. Effect of surface functionalization on the electronic transport properties of Ti_3C_2 Mxene. *Europhys. Lett.* **2015**, *111*, 67002. [CrossRef]
39. Sarikurt, S.; Cakır, D.; Keceli, M.; Sevik, C. The influence of surface functionalization on thermal transport and thermoelectric properties of MXene monolayers. *Nanoscale* **2018**, *10*, 8859–8868. [CrossRef]